DESIGN AND EXPERIMENTATION OF A MACHINE VISION-BASED QUALITY INSPECTION SYSTEM FOR GREEN ONION SEEDING
/
基于机器视觉的大葱播种质量检测系统的设计与试验

Fangyuan LU[1)], Chong TAO[2)], Zhiye MO[1)], Mengqi ZHANG[1)], Guohai ZHANG*[1)], Xiangyu WU[1)], Bolong WANG*[1)]
[1)] School of Agricultural Engineering and Food Science, Shandong University of Technology, Zibo/ China
[2)] Binzhou Polytechnic, Binzhou/ China
Tel: +8615965534882; +8613581044910; E-mail: guohaizhang@sdut.edu.cn; 892460540@qq.com;
Corresponding author: Guohai ZHANG, Bolong WANG
DOI: https://doi.org/10.35633/inmateh-74-19

Keywords: *Green onion seed, Machine vision, Primary concave defect segmentation algorithm, BP neural network, seeding quality detection*

ABSTRACT
In response to the inefficiency and low accuracy issues of traditional detection algorithms in detecting the tray seeding process of green onions, this paper proposes a machine vision-based quality inspection system for green onion seeding. Considering the color characteristics of green onion seeds and the substrate soil, the original RGB images are converted into HSV images. The HSV color filtering algorithm is employed to separate green onion seeds from complex soil backgrounds. Image noise is removed using erosion-dilation operations and small-area methods. The projection method is utilized to determine the detection area of the tray and the position of the holes. Information about connected regions and their convex hulls is extracted, and eight feature parameters including perimeter, area, shape factor, perimeter ratio, area ratio, shape factor ratio, concave defect distance ratio, and error variance are used to establish a BP neural network for single and adherent seed classification. A concave point segmentation algorithm is used to separate adherent green onion seeds and count the number of green onion seeds in each hole to obtain seeding quality parameters of the seeder. Experimental results show that the average relative error of the system qualification rate is 2.24%, with maximum and minimum relative errors of 3.22% and 1.10%, respectively. The average absolute errors of the reseeding rate and void rate are 1.31% and 0.71%, respectively. The absolute error of the average number of particles is 0.025 particles, the overall accuracy rate of the integrated seeding quality detection is 98%，and the average processing time per image is 0.91 s. The research results provide reference data for precision seeding operations of green onion seeders.

摘要
针对传统的检测算法在检测大葱秧盘播种过程中，效率低下，检测精度低等问题，本文提出了一种基于机器视觉的大葱播种质量检测系统。针对大葱种子颜色和基质土壤的颜色特征，将原始 RGB 图像转换成 HSV 图像。通过 HSV 色彩过滤算法将大葱种子从复杂的土壤背景中分离。使用腐蚀膨胀操作以及小面积法去除图像噪声。使用投影法确定秧盘检测区域和穴孔位置。提取连通区域及其凸包的信息，使用了周长、面积、形状因子、周长比、面积比、形状因子比、凹缺陷距离比、误差方差 8 个特征参数，建立 BP 神经网络单粒种子与粘连种子分类模型。使用凹点分割算法将粘连的大葱种子分离，并统计每穴大葱种子数量，得到排种器的播种质量参数。试验结果表明，系统合格率的平均相对误差为 2.24%，最大和最小相对误差分别为 3.22%和 1.10%；重播率和空穴率的平均绝对误差分别为 1.31%和 0.71%；平均粒数的绝对误差为 0.025 粒、综合播种质量检测准确率为 98%、每幅图像平均处理时间为 0.91 s。研究结果为大葱排种器精密播种作业提供了参考数据。

Fangyuan LU, As. Ph.D. Eng; Chong TAO, M.S. Stud. Eng.; Zhiye MO, M.S. Stud. Eng; Mengqi ZHANG, M.S. Stud. Eng.; Guohai ZHANG, As. Ph.D. Eng; Xiangyu WU, M.S. Stud. Eng.; Bolong WANG, As. Ph.D. Eng;

INTRODUCTION

As a biennial herb of allium in Liliaceae, green onion has high medical and economic value and has a long planting history in China. Additionally, it serves as a common vegetable and seasoning. With the increasing market demand, both the production and cultivation area of green onions have been steadily increasing year by year *(Wang et al.2019; Liu et al., 2017)*. Currently, field seedling cultivation of green onions heavily relies on manual labor, resulting in low efficiency and high labor intensity. Hence, there is a need to promote mechanized planting of green onions. In the mechanized planting process of green onions, according to the agronomic planting requirements of green onion seedling trays, most adopt a seeding scheme of 1-3 seeds per hole *(Peng et al., 2017)*. However, existing mechanical seeders for green onions often encounter problems such as missed seeding and reseeding due to various factors, significantly impacting the seedling quality of green onion trays. Therefore, it is of great significance to inspect the seedling quality of green onion trays to promptly adjust seeding devices and enhance the production performance of green onion seedling production lines.

In the current research, methods such as manual counting, photoelectric counting and machine vision are usually adopted for the detection and evaluation of crop seeding quality *(Zhang et al., 2022)*. Most of the traditional seed detection methods for crop seeding quality are carried out manually. In this way, after a long period of work, human eyes are easily tired, which inevitably leads to counting errors and cannot ensure accuracy *(Lv et al., 2023)*. Therefore, the study of replacing artificial testing of seeding quality and performance of crops has attracted widespread attention from researchers at home and abroad *(Li et al., 2022)*. At present, the technology that replaces manual detection is photoelectric technology and machine vision technology for detection. *Song et al., (2011),* designed and developed ZPXG-18 automatic photoelectric particle count meter and 1000-particle weight meter based on the newly discovered rotary disc inclined scraping principle, which allows for automatic particle sorting and separation. Let the disordered particles or seeds enter the groove tray with inclined grooves and arc grooves, driven by the bottom turntable to be diagonally scraped and shifted, automatically ordered and generated grain spacing, to obtain the reliable light transmission gap required by photoelectric counting, and to count the particles by presetting and rechecking the secondary counting. *Dong et al., (2019),* developed a real-time online monitoring system for seeding performance of hybrid rice based on embedded machine vision and machine learning technologies. By scanning the outline of each image to check whether there are seeds in the nest, the number of holes is calculated, and then the deficiency rate of hybrid rice is calculated. *Bai et al., (2021),* proposed a sweet corn seed detection method based on a voting mechanism to detect missing seeds in moving insert tray, replacing manual detection and improving the accuracy of corn seeding detection. *Tan et al., (2019),* proposed the integral segmentation and counting method, which tested three hybrid rice varieties and realized the evaluation of seeding performance. At present, most of the researches are focused on the seeds of large grain crops such as rice and corn, but there are few researches on the sowing quality detection of small grain and irregular green onion seeds. Compared to traditional manual counting and photoelectric counting methods, the seeding detection technology based on machine vision demonstrates superior efficiency and accuracy when handling complex detection scenarios. Therefore, researching and developing a machine vision-based quality detection system for green onion sowing holds significant importance.

In this paper, a detection method based on machine vision and BP neural network is proposed to detect the seeding quality of scallion seedling tray. Firstly, a machine vision image acquisition platform is constructed to capture images. Then, the image processing algorithm is used to process the seed images of green onion in different soil environments. Finally, the seeding quality detection algorithm is designed based on BP neural network and main concave defect segmentation algorithm, and the experiment is verified.

MATERIAL AND METHODS

Testing system

The test system was installed on the precision scallion seedling feeder developed by the College of Agricultural Engineering and Food Science of Shandong University of Technology, and the scallion seeding quality detection system based on machine vision and BP neural network was set on the conveyor belt after the seedling tray was sown. The system is mainly composed of a computer, a light box, a high-definition industrial camera, and a network cable, as shown in Fig. 1.

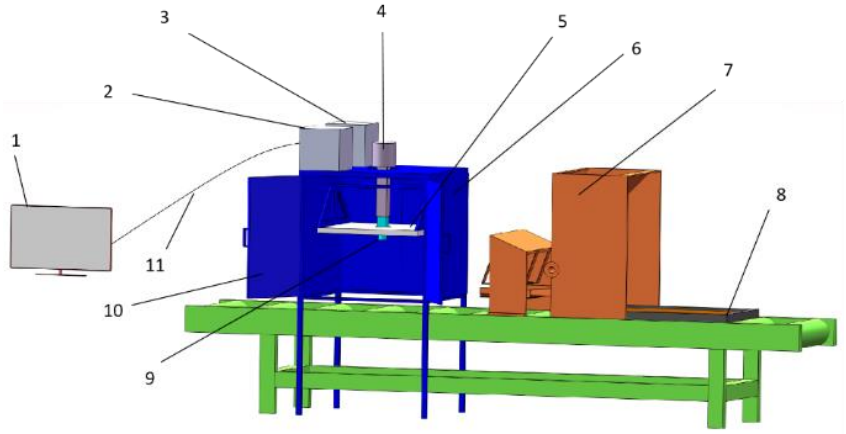

Fig. 1 - Schematic diagram of green onion sowing quality inspection system

1 – Light box; 2 - Light source; 3 - Network cable; 4 - Computer; 5 - Green onion seed; 6 - Rice seedling tray; 7 - High-definition industrial camera; 8 - Tray; 9 - Industrial camera; 10 - Light box door; 11 - Tata transmission line

The computer uses the DELL G15 5515, which is configured with a 3.30 GHz CPU and 16GB of baseband RAM. The light box uses stainless steel as the shell, and has a 600 mm×600 mm hole surface light source, and the camera passes through the hole. High-definition industrial cameras use the Keenes series CA-HF2100C, lens model CA-LHE12. When shooting, the computer uses a USB cable to control the high-definition industrial camera for shooting work. The size of the test seedling tray was 580 mm×280 mm, in which there were 12 holes in each row and 23 holes in each column. By adjusting the mounting height of the camera, the shooting range in the camera window is approximately 9×11 holes during each shooting.

Image preprocessing

The seedling plate images acquired by high-definition industrial cameras are RGB images, as shown in Fig. 1, in which the color of green onion seeds is black. In order to meet a wider application range, two kinds of soil were selected as the background soil of green onion seeds in this experiment, one is the matrix soil for cultivating vegetables, and the other is the planting soil from the planting area of green onion, as shown in Fig.2.

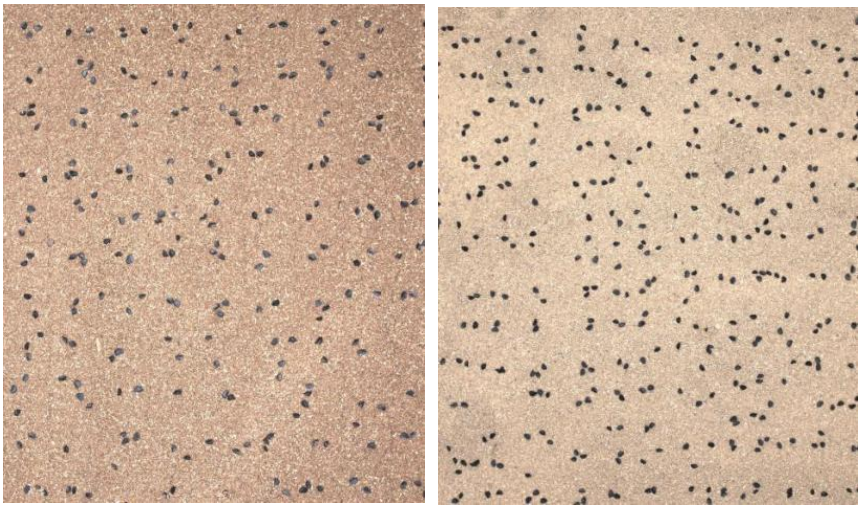

(a) *(b)*

Fig. 2 - Captured RGB original image. (a) matrix soil; (b) Planting soil

In order to separate the green onion seeds from the complex soil background, the RGB image was first transferred into the HSV color space for processing. The resulting processed image was shown in Fig. 3.

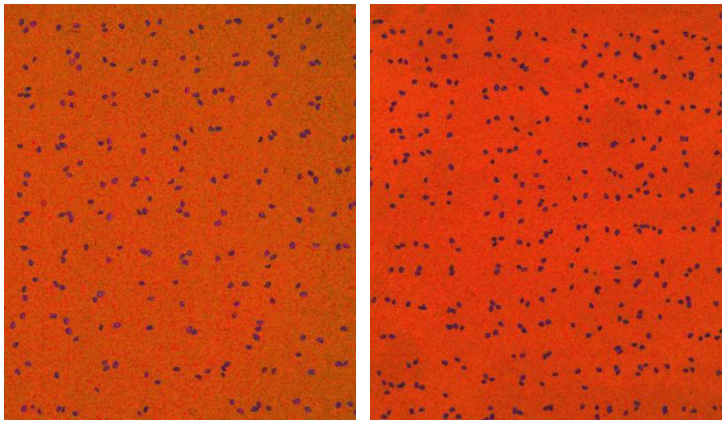

(a) *(b)*

Fig. 3 - HSV color space image. (a) Matrix soil; (b) Planting soil

The experiment showed that after converting the acquired RGB image into an HSV image, the color of green onion seeds could be distinguished from the background soil, allowing for the effective extraction of the target objects. In the HSV color space, the color of green onion seeds differs significantly from the background soil color, enabling the initial extraction of green onion seeds by isolating specific color regions in the HSV space (*Ren et al., 2021*). Additionally, due to the physical characteristics of the seeds or the presence of reflective phenomena, the color of scallion seeds in the HSV space image varies, as illustrated in Fig. 4.

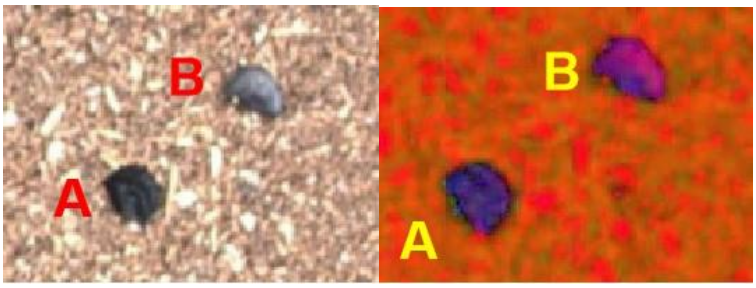

(a) *(b)*

Fig. 4 - Color of different green onion seeds. (a) RGB image ; (b) HSV image

Therefore, it was also necessary to obtain the best color interval through the experiment. In order to meet the goal of better extraction of green onion seed image under two soil backgrounds at the same time, it was necessary to determine the value range of H (hue), S (saturation) and V (value) of green onion seed in HSV image. EVENT_LBUTTONDOWN function and click callback function could be used to collect HSV parameters of the points of green onion seeds in the soil background from HSV images, as shown in Fig. 5. The coordinates of the collected pixels were indicated in parentheses, and the parameter values of H, S, and V are also provided in parentheses.

```
HSV value at position (1248, 254): [133  36  49]
HSV value at position (1435, 291): [140  13  61]
HSV value at position (1543, 298): [111  50  51]
HSV value at position (1230, 505): [156  14  94]
HSV value at position (1221, 512): [104  49  99]
HSV value at position (1207, 506): [108  56  78]
HSV value at position (1265, 478): [101  57  76]
HSV value at position (1541, 471): [111  52  64]
HSV value at position (1550, 481): [120  30  85]
HSV value at position (1261, 601): [120  13  40]
HSV value at position (1262, 607): [75  9 56]
```

Fig. 5 - Process diagram of collecting HSV information

Among H, S and V, H was the most important for color expression. The analysis of H value parameters of green onion seeds under the two soil backgrounds provided an important reference for extracting target images of green onion seeds. By collecting the color parameters of 2000 green onion seed pixels, the value range of H parameter could be obtained as shown in the following table.

Table 1

H value of green onion seeds under different soil background

Parameter	H minimum value	H maximum value	H mean value
Substrate soil as the background	42	140	115
The local loess is the background	47	149	122

Based on the H parameter of scallion seeds under the two soils, the optimal H value range for the target of extraction of scallion seeds was obtained through experiments as [42,169]. Moreover, there was no obvious difference between the S value and V value in the seed and soil background of green onion, so the value interval of S value and V value was set to the maximum range [0,255]. After defining the color value range of green onion seeds in the HSV space, the binary mask was created by the cv2.inRange function, as shown in Fig. 6.

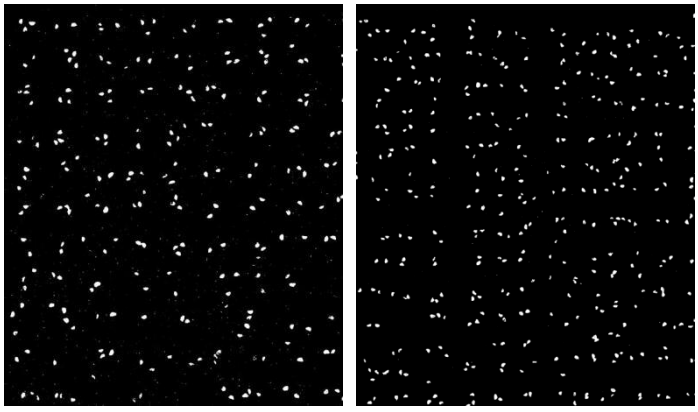

(a) *(b)*

Fig. 6 - Binary mask image. (a) Matrix soil; (b) Planting soil

At this time, there were many small noise points in the image, so it was necessary to de-noise the image. Taking the matrix soil with more noise points as an example. Therefore, the binary mask was corroded and expanded, and large noise points in the image were removed by small area method. After processing by the above method, noise points in the image could be effectively filtered out, and finally the seedling was located by projection method, the processing results were shown in Fig. 7.

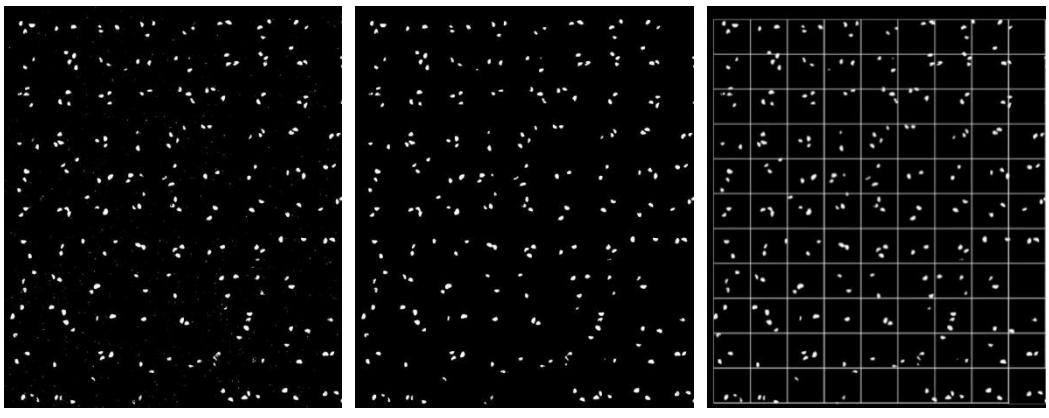

(a) *(b)* *(c)*

Fig. 7 - Images before and after noise reduction

(a) Original drawings; (b) Images after noise reduction; (c) Projection of legal post-image

The formula for corrosion expansion operation was as follows:

Corrosion operation:

$$(E(A,B))(x,y) = min_{(i,j)\in B} A(x+i, y+j) \quad (1)$$

Expansive working:

$$(D(A,B))(x,y) = max_{(i,j)\in B} A(x+i, y+j) \quad (2)$$

where:

$E(A,B)$ - Etch operation; $D(A,B)$ - Expansive working; A - Input image; B - Structural element; (x,y) - Pixel position in the image; (i,j) - Relative coordinates within structural elements; max - Take the maximum value of the corresponding pixel in all structure elements in B; min - Take the minimum value of the corresponding pixel value in all structure elements in B.

Eigenvalue extraction

In the process of seeding, there would be a phenomenon of multi-grain adhesion of green onion seeds, which would make the image recognize multiple seeds into one grain during the contour recognition and counting process, thus affecting the accuracy of seeding detection.

Therefore, it was necessary to first classify the adhered multi-seed and single seed, and then segment the adhered seeds. In this study, BP neural network *(Sun et al., 2022)* was used to extract the adhered multi-seed, and the eigenvalue should be determined first.

In this study, three parameters, perimeter C_1, area S_1 and form factor SF_1, were selected as the shape features of green onion seeds, and five parameters, perimeter ratio P_r, area ratio A_r, error variance V_e, shape factor ratio S_r and concave defect distance ratio C_r, were selected as the external convex hull features as input values of BP neural network. For the single and multi-grain scallion seeds, the shape characteristics of the connected domain of scallion seeds in the simply connected domain were calculated, as shown in Table 2. The characteristic parameters of external convex hull of single and multi-grain adhesive green onion seeds were shown in Table 3.

Table 2

Simple connected region shape characteristics of different number of green onion seeds

Parameter	Shape characteristics of simple connected region of green onion seeds with different seed numbers		
Number	**1**	**2**	**3**
Perimeter (pixels)	161	314	357
Area (pixels)	1505	3278	3757
Shape factor	0.72	0.41	0.37

Table 3

The characteristics of the outer convex envelope in the simply connected region of different number of green onion seeds

Parameter	Characteristic statistics of different number of green onion seeds with outer convex hull		
Number	**1**	**2**	**3**
Perimeter ratio	1.03	1.34	1.481
Area ratio	0.93	0.72	0.65
Error variance	0.55	45.23	76.93
Form factor ratio	0.80	0.53	0.33
Concave defect distance ratio	0.13	5.74	8.34

Construction of BP neural network

BP neural network was a multi-layer feedforward neural network based on error calculation, and its weight was adjusted according to the error backward propagation algorithm in order to achieve continuous

error reduction. This process was similar to calculating the error through a forward neural network and then backpropagating to adjust the weight of the neuron until the error is minimized *(Deng et al., 2022)*. In this study, the input layer of BP neural network was set with 8 neurons, representing 8 characteristic parameters. The output layer was set up with two neurons, one representing a single seed and one representing multiple seeds. This allows you to distinguish single seeds from multiple seeds. The performance of BP neural network was affected by the number of neurons in the hidden layer, and the number of neurons in the hidden layer was usually determined by a large number of tests and experiences. The empirical formula was expressed as formula 3.

$$NUM = \sqrt{p + q} + b \tag{3}$$

where:

NUM - Number of hidden layer neurons; p - Enter the number of layer vectors; q - Output the number of layer vectors; b - Adjustable empirical constant, the value range was [1,10].

In this paper, the traditional BP neural network was selected for training comparison with the optimized BP neural network. The optimized transfer function was Leaky ReLU, and the output layer transfer function was Purelin. The Adaptive Moment Estimation algorithm was used to train the deep neural network *(Zhang et al., 2022)*.

Data set construction

Through image preprocessing, the binarized connected domain images of scallion seeds were extracted from the complex background. A total of 3602 images were obtained, including 2750 single scallion seeds and 852 multi-scallion seed images *(Ding et al., 2019)*. In order to enhance the training effect and generalization performance of the model, methods such as amplification, rotation and noise increase were used to expand the data set. After expansion and processing, the data set has a total of 6033 images. The two kinds of pictures of single scallion seed and multi-scallion seed adhesion were used as the training set and the test set of BP neural network according to the ratio of 3:1:1. The dataset image was shown in the Fig. 8.

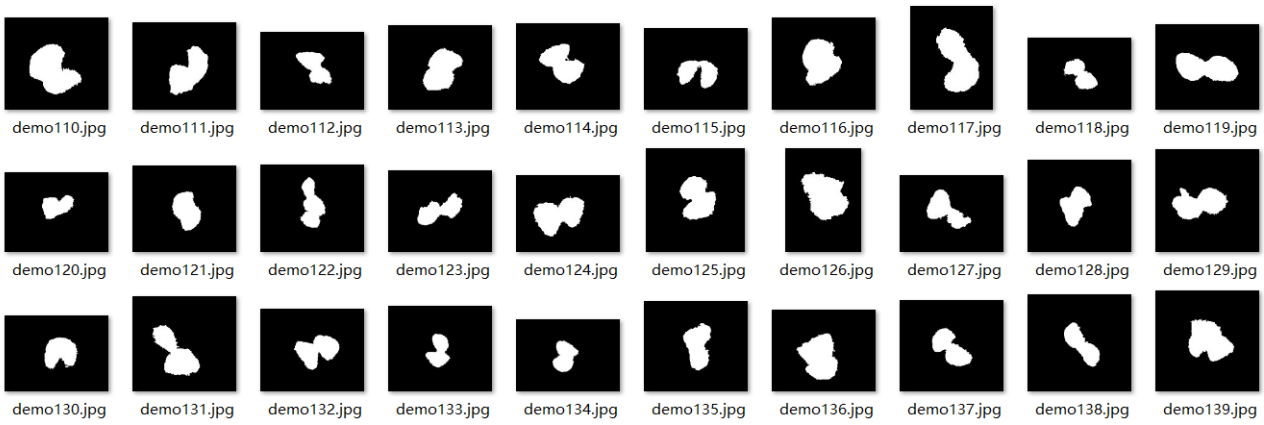

Fig. 8 - Dataset image

Main concave defect segmentation algorithm

On the edge or inside of a polygon, a line segment connecting two points can always be found. This polygon encompasses all points, and the smallest such polygon is termed a convex hull. For a geometry, the outer convex hull is a convex polygon whose boundary completely encloses all points within the given geometry. A concave defect represents a dip or void in the outline shape of an object. A concave point is a point that forms the boundary of a concave defect. The red dot in the figure identifies the concave spot on the image, the green line outline represents the outer convex envelope of the scallion seed, and the yellow area highlights the main concave defect area. Points D, E and F represent the starting point, the deepest point and the ending point of the largest concave defect area of the adhesive allium seeds, respectively. The other red pits in the image also represent the deepest point of the small concave defect, and each pit can be the deepest point of the concave defect, the starting point and the ending point, so the number of pits was equal *(Zhu et al., 2023)*.

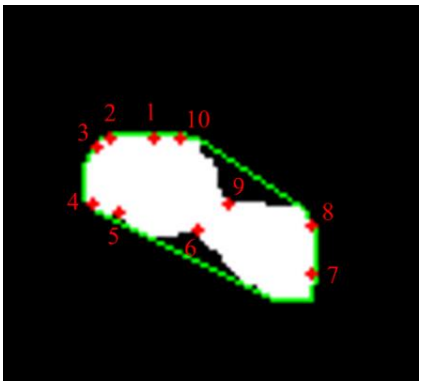

Fig. 9 - Concave detection sequence

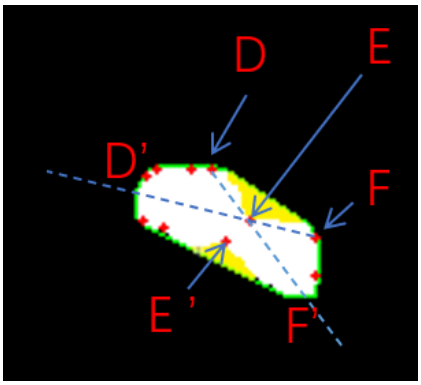

Fig. 10 - Principle diagram of main concave defect segmentation

There is no concave defect in the outer convex hull of single scallion seeds. However, for the multi-grain seeds, the outer convex hull has concave defects. It is necessary to use concave defect segmentation algorithm to divide these adhered onion seeds into single seeds. The determination of the concave defect depth threshold is critical. A lower threshold may lead to misidentification of minor concavities on the green onion seed surface as connection points between two seeds, resulting in erroneous segmentation. Conversely, an excessively high threshold may cause omission of key segmentation points, leading to missed segmentation. Therefore, it is imperative to select an appropriate concave defect depth threshold. Extensive preliminary experiments have determined that setting the concave defect depth threshold to 5.23 yields the highest accuracy in segmenting images of adhered green onion seeds *(Nicolau et al., 2023)*.

For the adhesive onion seeds, the workflow of image segmentation proposed in this study was as follows, illustrated by Fig. 10:

(1) Traversal and selection of main segmentation points: The system first traverses all concave points in the image to find the concave defect point with the greatest depth. By comparing the concave defect depth of this point with the size of the concave defect depth threshold 5.23, if the concave defect depth was greater than the threshold, this point (such as point E in Fig. 9) was identified as the main concave point of segmentation. If the depth of the concave defect was less than the threshold, the process stopped the current segmentation operation and moved to the next connected domain of the onion seed for detection.

(2) Determination of the secondary split point: Then, by extending the DF and EF line segments, an included angle ∠D'EF' was formed, as shown in Fig. 9. In this specific region, the concave defect point with the largest depth was selected as the secondary segmentation point, and the deepest concave point in this region was the E' point. The image segmentation operation was completed by connecting EE'. If no concave point was found in the area of the included angle, the point closest to point E in the area of the included angle ∠D'EF was selected as the segmentation point. This point was usually the narrowest part of the seed outline, ensuring effective segmentation based on physical form in the absence of significant concave defects.

(3) Repeated adhesion detection and segmentation: The segmented image was tested for adhesion again. If there was still adhesion, Step 1 was performed again to continue the division of the adhesive seeds. If no adhesion was detected, the process proceeded to the detection of the connected domain of the next onion seed. The effect of the segmentation was shown in Fig. 11.

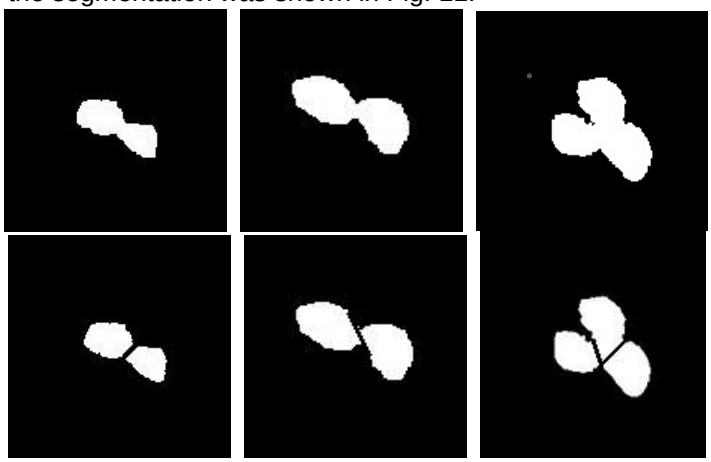

Fig. 11 - Adhesive seed segmentation effect

Field test

The image collection was carried out after the soil was covered and sown on the seedling tray, which was then moved to the image collection area by a conveyor belt. The speed of the conveyor belt was set to 600 plates per hour to ensure that when the plate enters the shooting area of the camera, the camera could cover 9×11 holes of the window, meaning each image contained 99 seedling holes. The camera shooting interval was set to 2.9 s, ensuring each seedling plate was shot twice, and each shooting area did not overlap. The average processing time of each image was 0.91 s, and the hole rate, pass rate, reseeding rate and average grain number were calculated. The error rate of test results was shown in Table 4. Finally, the number of green onion seeds in each hole in the seedling plate image was output. Among them, 0 seeds in each point were classified as empty point sowing, 1-3 seeds in each point were qualified, and 3 seeds in each point were repeated.

RESULTS

BP neural network training results

In this study, the traditional BP neural network architecture and the optimized BP neural network architecture were used for training. After 100 training cycles (epochs), the loss and accuracy trends of the two models were shown in Fig. 12.

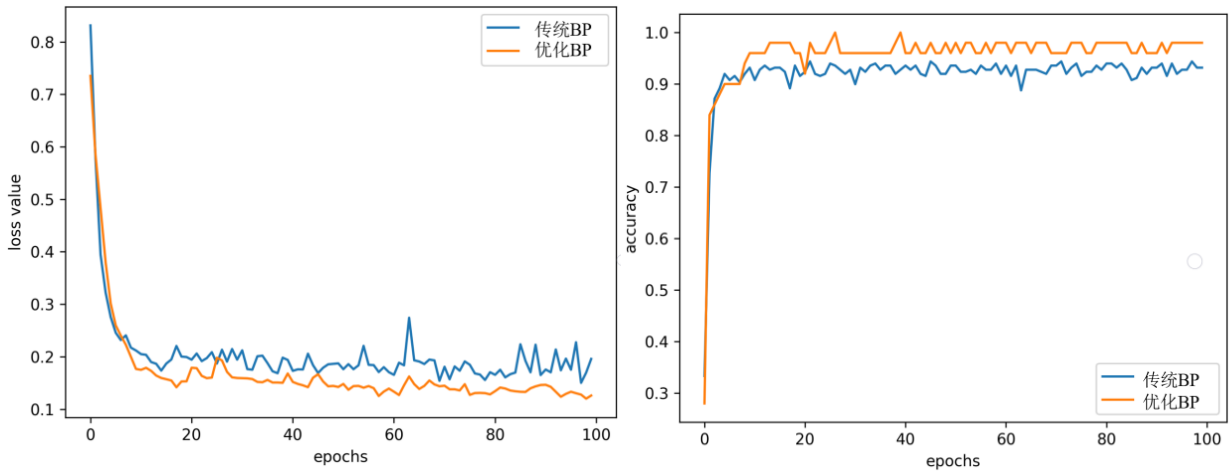

(a) *(b)*

Fig. 12 - Loss rate versus accuracy rate. (a) Loss ratio; (b) Accuracy rate

It can be seen from Fig. 12(a) that after completing 20 iterations, the loss rate and accuracy of the two neural network models tend to converge basically. The loss rate of traditional BP neural network tends to be stable, in the range of about 0.19, but in the subsequent training process, the loss rate fluctuates significantly. In contrast, the optimized BP neural network showed a decreasing trend of loss rate after 20 iterations, and the final loss rate stabilized at about 0.14, and the corresponding fluctuation range was smaller, showing higher stability than the traditional BP neural network.

In terms of accuracy, as shown in Fig. 12(b), after iterative convergence, the classification accuracy of the traditional BP neural network was stable at about 93%, while the classification accuracy of the optimized BP neural network was stable at 98%. The performance of the optimized BP neural network continues to outperform the traditional BP neural network after convergence, especially in the later stage of training. The accuracy curve of the optimized model showed the advantage of higher stability and continuity.

The optimized BP neural network exhibits a lower loss rate, indicating that the gap between the model's predictions and the actual values has narrowed, thus improving prediction accuracy. Additionally, the increased accuracy reflects the model's enhanced ability to precisely distinguish between different categories in classification tasks. Overall, these improvements clearly demonstrate that the optimized BP neural network outperforms its pre-optimized version.

Field test verifies the results

In order to verify the accuracy of the system, a field test was carried out in the agricultural machinery greenhouse of Shandong University of Technology, as shown in Fig.13.

Fig. 13 - Field test

The error rates of qualified rate, replay rate, hole rate and average number of grains were obtained by comparing system detection with manual detection, as shown in the Table 4.

Table 4

The relative error rate of system and manual inspection

Number	Pass rate (%)	Replay rate (%)	Hole rate (%)	Average number of grains (grains)
	Relative error	Absolute error	Absolute error	Absolute error
1	2.15	2.02	0	0.02
2	2.17	1.01	1.01	0.02
3	2.10	2.02	0	0.03
4	1.10	0	1.01	0.02
5	2.08	1.01	0	0.04
6	3.19	2.02	1.01	0.03
7	1.12	1.01	0	0.03
8	2.06	1.01	1.01	0.01
9	3.22	1.01	2.02	0.02
10	3.16	2.02	1.01	0.03
Average error rate	2.24	1.31	0.707	0.025

Through the above experiments, the results of the seeding quality detection system and manual detection method were compared in this paper. In the measurement of pass rate, replay rate, hole rate and average number of grains, the system's detection errors were all within the acceptable error range. Specifically, the average relative error of the pass rate was 2.24%, the maximum relative error was 3.22%, and the minimum relative error was only 1.10%. The average absolute error value of the replay rate was 1.31%, and the average absolute error value of the hole rate was 0.71%. The absolute error of the average number of grains was 0.025 grains. According to the comprehensive index, the seeding quality detection system had high accuracy, and its detection speed was significantly better than the traditional manual detection method. Therefore, the system could effectively replace the manual inspection of green onion sowing quality, reduce the consumption of human resources, and improve the working efficiency.

CONCLUSIONS

(1) Design and hardware construction of the quality inspection system for scallion seedling and sowing on the scallion seedling tray: According to the size of the scallion precision seeder and the size of the scallion seed, a set of hardware image acquisition platform was built. These mainly include light boxes, light sources, cameras, lenses, and computers. Selecting the appropriate hardware could make the acquired image clearer, with higher contrast, which provided convenience for image processing.

(2) Image preprocessing and seed target extraction: A method was proposed to detect the seed quality of green onion in various soil environments. This method compared the two soil environment images in RGB and HSV color space, and found that the HSV space was more conducive to extraction of green onion seed targets. The fixed double threshold method was used to extract the green onion seed targets in HSV images, and the corrosion expansion method and small area method were used to enhance the images.

(3) Research on seeding quality detection algorithm: A method based on BP neural network was proposed to classify single seed and multiple adhered seeds. The classification model of single seed and adherent seed was successfully constructed by using 8 characteristic parameters, such as perimeter, area, shape factor, perimeter ratio, area ratio, error variance, shape factor ratio and concave defect distance ratio. In the training stage of BP neural network, the dataset was constructed, and data augmentation methods were applied to expand the dataset. The prediction performance of BP neural network was evaluated. The main concave defect segmentation algorithm was used to segment the adhered seeds, and the kernel method was used to judge the seed site belonging to the seeds on the seedling site line. Finally, the seeding quality of the whole image was assessed through a large number of seed quality testing experiments of green onions.

(4) Experimental verification: In the process of experimental verification, it was concluded that the average relative error between the qualified rate of system detection and manual detection was 2.24%. The maximum relative error was 3.22%, and the minimum relative error was 1.10%. Additionally, the average absolute error value of replay rate was 1.31%, and the average absolute error value of hole rate was 0.71%. The absolute error of average number of grains was 0.025 grains. The overall accuracy rate of the integrated seeding quality detection is 98% . The detection time of each image was 0.91 s.

ACKNOWLEDGEMENT

This research was supported by the Key Research and Development Project of Ningxia Hui Autonomous Region (2023BCF01052).

REFERENCES

[1] Bai, J., Hao, F., Cheng, G., Li, C. (2021). Machine vision-based supplemental seeding device for plug seedling of sweet corn. *Computers and Electronics in Agriculture*, Vol. 188, pp. 106345.

[2] Deng, X., Zhang, S., Shao, Y., Yan, X. (2022). A real-time sheep counting detection system based on machine learning. *INMATEH-Agricultural Engineering*, Vol. 67, Issue 2, pp. 85-94.

[3] Ding, A., Zhang, X., Zou, X., Qian, Y., Yao, H., Zhang, S., Wei, Y. (2019). A novel method for the group characteristics analysis of yellow feather broilers under the heat stress based on object detection and transfer learning. *INMATEH-Agricultural Engineering*, Vol. 59, Issue 3, pp. 49-58.

[4] Dong, W., Ma, X., Li, H., Tan, S., Guo, L. (2019). Detection of performance of hybrid rice pot-tray sowing utilizing machine vision and machine learning approach. *Sensors,* Vol. 19, Issue 23, pp. 5332.

[5] Li, Y., Xiao, L., Li, W., Li, H., Liu, J. (2022). Research on recognition of occluded orange fruit on trees based on YOLOv4. *INMATEH-Agricultural Engineering*, Vol. 67, Issue 2, pp. 137.

[6] Liu D., Gao H., Wang F., & Zhou J., (2017). Planting Agronomy and Mechanization Production Technology of Scallion in Zhangqiu (章丘大葱种植农艺及机械化生产技术), *Transactions of Agricultural. Engineering*, Vol.7, Issue.1, pp.15-18+47.

[7] Lv, Z., Zhang, W., Zeng, X., Han, Y., (2023). Design and experiment of potato seedling film-breaking device based on machine vision. *INMATEH-Agricultural Engineering*, Vol. 71, Issue 3, pp. 136.

[8] Nicolau M.M., Alcover G.M., Hidalgo M.G., Jaume-i-Capo A. (2023). Improving concave point detection to better segment overlapped objects in images. *Multimedia Tools and Applications*, Vol.83, Issue 8, pp. 24339-24359.Peng S, Yang Y, Chen, L, Jiang Z., (2017). Analysis on planting and mechanized harvesting of Welsh onion (大葱种植与机械化收获分析), *Transactions of Journal of Chinese Agricultural Mechanization*, Vol.38, issue.9, pp.30-35.

[9] Ren, X., Wang, H., Shi, X. (2021). Research on visual navigation path detection method for dense plum grove. *INMATEH-Agricultural Engineering*, Vol. 65, Issue 3, pp. 111.

[10] Song R.S., Lan J.Z., Xia S.F., Hua J., (2011). Design of ZPXG-18 photoelectric instrument to automatically count and weigh up to 1 000 granules (ZPXG-18 型转盘斜刮式自动光电数粒仪和千粒重仪的设计), *Transactions of Acta Agriculturae Zhejiangensis*, vol.23, issue.5, pp.1023-1028

[11] Sun, B., Mu, D., Dou, W., Sun, S., Jiang, M. (2022). Designing an intelligent irrigation system by using backpropagation neural network to predict water demand. *INMATEH-Agricultural Engineering*, Vol. 67, Issue 2, pp. 525-532.

[12] Tan, S., Ma, X., Mai, Z., Qi, L., Wang, Y. (2019). Segmentation and counting algorithm for touching hybrid rice grains. *Computers and Electronics in Agriculture*, Vol. 162, pp. 493-504.

[13] Wang H.X., Wu Y.Q., Li T.H., Zhang J.Q., & Hou J.L. (2019). Current situation and prospect of research on Welsh onion planting machinery (大葱种植机械研究现状与展望), *Transactions of Journal of Chinese Agricultural Mechanization*, Vol.40, Issue.2, pp.35-39.

[14] Zhang, X., Hou, Z., Xuan, C., (2022). Design and experiment of recognition system for coated red clover seeds based on machine vision. *INMATEH-Agricultural Engineering*, Vol. 66, Issue.1, pp. 62-72.

[15] Zhang, W., Han, Y., Huang, C., Chen, Z. (2022). Recognition method for seed potato buds based on improved YOLOv3-tiny. *INMATEH-Agricultural Engineering*, Vol. 67, Issue 2, pp. 364-373.

[16] Zhu, Y., Wang, H., Li, Z., Zhen, T. (2023). Detection of corn unsound kernels based on GAN sample enhancement and improved lightweight network. Journal of Food Process Engineering, Vol. 47, Issue 1.